

# V<sup>2</sup>Flow: Unifying Visual Tokenization and Large Language Model Vocabularies for Autoregressive Image Generation

Guiwei Zhang<sup>1</sup>, Tianyu Zhang<sup>1</sup>, Mohan Zhou<sup>1</sup>, Yalong Bai<sup>1\*</sup>, Biye Li<sup>1</sup>

<sup>1</sup> Du Xiaoman Financial.

{zhangguiwei0610, tianyu1949, libiye}@gmail.com {mhzhou99, ylbai}@outlook.com

## Abstract

We propose V<sup>2</sup>Flow, a novel tokenizer that produces discrete visual tokens capable of high-fidelity reconstruction, while ensuring structural and latent distribution alignment with the vocabulary space of large language models (LLMs). Leveraging this tight visual-vocabulary coupling, V<sup>2</sup>Flow enables autoregressive visual generation on top of existing LLMs. Our approach formulates visual tokenization as a flow-matching problem, aiming to learn a mapping from a standard normal prior to the continuous image distribution, conditioned on token sequences embedded within the LLM’s vocabulary space. The effectiveness of V<sup>2</sup>Flow stems from two core designs. First, we propose a Visual Vocabulary resampler, which compresses visual data into compact token sequences, with each represented as a soft categorical distribution over LLM’s vocabulary. This allows seamless integration of visual tokens into existing LLMs for autoregressive visual generation. Second, we present a masked autoregressive Rectified-Flow decoder, employing a masked transformer encoder-decoder to refine visual tokens into contextually enriched embeddings. These embeddings then condition a dedicated velocity field for precise reconstruction. Additionally, an autoregressive rectified-flow sampling strategy is incorporated, ensuring flexible sequence lengths while preserving competitive reconstruction quality. Extensive experiments show that V<sup>2</sup>Flow outperforms mainstream VQ-based tokenizers and facilitates autoregressive visual generation on top of existing.

## 1. Introduction

Autoregressive modeling has recently emerged as a prominent paradigm in both natural language processing [2, 8, 42] and multimodal understanding [5, 25, 50, 56, 60], advancing the integration of visual perception with linguistic inter-

faces. Building upon these successes, an increasing body of work [7, 11, 12, 37, 38] has begun to explore autoregressive modeling for visual generation. Although promising, these approaches [12, 38, 46, 47, 59] operate under a paradigm that representing language in a discrete, categorical form [42], while modeling visual information within continuous feature spaces [18, 30], i.e., equipping LLMs with the power of diffusion models [14, 34]. This representational discrepancy introduces additional architectural complexity and computational overhead, preventing autoregressive visual generation from attaining the streamlined efficiency seen in language tasks.

Recent research [19, 36, 40, 53] has explored one promising solution: leveraging a single transformer architecture to unify visual and textual data within the next-token prediction framework. In this paradigm, visual content is quantized into discrete tokens [9, 21, 52, 58] that can be jointly processed alongside categorical, discrete textual data for autoregressive visual generation. However, a fundamental challenge arises. Existing methods predominantly employ VQ-based tokenizers [9, 33] optimized solely for visual reconstruction, causing the distribution of discretized visual tokens to misalign with the semantically rich representations of text. Furthermore, existing approaches preserve the intrinsic two-dimensional structure of images, forcing autoregressive models to predict visual tokens in a line-by-line manner. This diverges sharply from the processing of one-dimensional textual data. Both structural and latent distribution disparities introduce competition between two modalities, thereby hindering the efficiency and effectiveness of unified autoregressive modeling [40].

These limitations reveal a critical gap within current autoregressive visual generation paradigms: the absence of a visual tokenizer capable of achieving both high-fidelity image reconstruction and effective latent distribution alignment with pretrained LLMs textual features. Addressing this gap is critical for effective multimodal integration and enhanced image-text association learning. Motivated by this, we pose a central question: *Can we design a visual tokenizer capable of generating discrete tokens that*

\*Project lead

<https://github.com/zhangguiwei610/V2Flow>

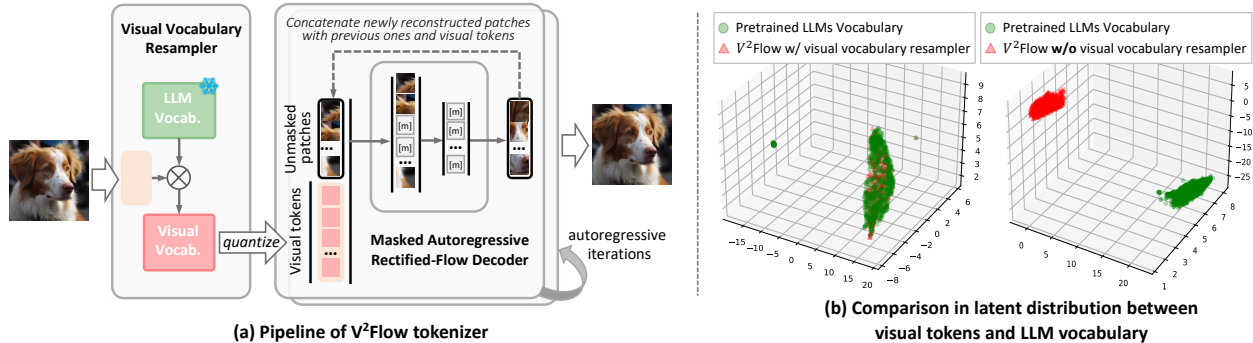


Figure 1. Highlights of  $V^2$ Flow tokenizer. In (a), a visual vocabulary resampler compresses visual content into a compact one-dimensional token sequence. Each token is directly expressed within the latent distribution of existing LLMs vocabulary space, as illustrated in (b). This design facilitates autoregressive visual generation on top of existing LLMs. Subsequently, the quantized visual tokens condition on a masked autoregressive Rectified-Flow decoder for high-fidelity visual reconstruction.

### achieve accurate reconstruction and seamless integration with pretrained LLMs’ vocabularies?

In response, we propose  $V^2$ Flow, a novel tokenizer designed to generate discrete tokens aligned structurally and in latent distribution with existing LLMs. Our key insight is to embed visual features directly into the vocabulary space of pretrained LLMs (e.g., the LLaMA series [8, 42]). This paradigm naturally situates visual representations within the existing text embedding space of LLMs, circumventing the need for forced semantic alignment. This effectively harmonizes visual and textual modalities, significantly alleviating challenges induced by discrepancies in their respective feature scales and distributions. Consequently, our approach facilitates efficient autoregressive image generation directly leveraging pretrained LLMs.

Although our  $V^2$ Flow operates with a quantized vocabulary of limited cardinality, we empirically demonstrate that this constraint does not restrict the representational capability. Instead, the expressive power of  $V^2$ Flow primarily emerges from the intricate interactions and rich co-occurrence patterns among visual tokens. Fine-grained visual details, particularly high-frequency structures, naturally arise through explicit modeling of token dependencies [13, 45]. Inspired by masked image modeling [13, 22], we introduced a targeted masked approach, designed to capture these critical co-occurrence patterns. Furthermore, we integrate this with Rectified-Flow sampling [10], effectively transforming discrete tokens into continuous distributions for high-quality visual reconstruction.

Fig. 1 highlights two primary designs of the  $V^2$ Flow tokenizer. **First**, to enforce structural alignment and latent distribution consistency between visual tokens and pretrained LLMs vocabulary, we propose a *visual vocabulary resampler*. This resampler compresses visual content into a compact one-dimensional token sequence, mapping each token into a soft categorical distribution over the LLM vo-

cabulary space. As illustrated in Fig. 1(b), visual tokens produced without our resampler exhibit latent distributions distinctly divergent from textual embeddings. In contrast, the tokens processed by our resampler exhibit latent distribution closely aligned with the LLM vocabulary. Both structural and latent distribution compatibility can significantly reduce complexity when integrating visual tokens directly into existing LLMs. **Second**, to refine quantized token sequences for high-fidelity reconstruction, we propose a *masked autoregressive rectified-flow decoder*. Inspired by recent advances in masked generative modeling, our decoder employs a masked transformer encoder-decoder design, enriching visual tokens with contextually rich information. These embeddings subsequently condition a dedicated velocity field model to reconstruct continuous visual distributions from a standard normal prior. During rectified-flow sampling, our decoder adopts an “next set-of-tokens” prediction strategy. Compared to prior tokenizers [55] that solely rely on masked encoder-decoder, this approach facilitates superior reconstruction quality with shorter token sequences, thereby improving overall compression efficiency. (Please see Sec. 3.2 for details). Our contributions include:

- We propose a visual vocabulary resampler that quantizes images into a compact one-dimensional sequence represented within the LLM vocabulary space. By leveraging these tokens, our tokenizer facilitates seamless autoregressive visual generation built upon existing LLMs.
- We develop a masked autoregressive rectified-flow decoder, equipped with an autoregressive sampling strategy. This design facilitates visual tokenization at flexible sequence lengths while preserving robust and competitive reconstruction quality.
- Extensive experimental results show that our  $V^2$ Flow tokenizer achieves competitive reconstruction performance compared to mainstream VQ-based tokenizers, and effectively promote autoregressive visual generation.

## 2. V<sup>2</sup>Flow tokenizer

### 2.1. Task Formulation and Overview

**Visual Tokenization from a Flow-Matching Perspective.** Our goal is to compress images into compact, one-dimensional sequences of quantized tokens. Each token is embedded within the vocabulary space of pretrained LLMs. This tokenization process must satisfy two essential criteria:

- *High-fidelity visual reconstruction.* The quantized tokens must preserve essential visual details to ensure faithful image reconstruction.
- *Structural and latent distribution alignment with LLMs.* Each visual token should be naturally integrated into LLMs vocabulary space, enabling autoregressive visual generation with minimal adjustments to existing LLMs.

To meet these requirements, we formulate visual tokenization as a flow-matching problem. In particular, we learn a mapping from latent variables  $\epsilon \sim \mathcal{N}(0, 1)$  to samples  $z$  from the visual data distribution  $q$ , via an ordinary differential equation (ODE),

$$dz_t = \psi_{\Theta}(z_t, t, \mathbf{V}^2) dt \quad (1)$$

where  $\psi_{\Theta}$  denotes a learnable velocity field parameterized by the weights  $\Theta$  of our tokenizer decoder, and  $t \in [0, 1]$  is the time-step. The term  $\mathbf{V}^2$  represents the quantized token sequence from our visual vocabulary resampler (see Sec. 2.2), which conditions the velocity field  $\psi_{\Theta}$  to guide the generation process. Each token in  $\mathbf{V}^2$  is directly represented within the LLMs vocabulary space. This effectively bridges the distribution gap between visual tokens and the LLM’s generative capability.

Directly solving the ODE in Eq. (1) with differentiable ODE solvers is computationally expensive. A more efficient alternative is to regress a time-dependent vector field  $u_t(z | \epsilon)$  that generates a probability path between  $\mathcal{N}(0, I)$  and the target distribution  $q$ . For optimization efficiency, we employ a rectified-flow [10], in which the trajectory between the target distribution and standard normal distribution is assumed to follow a “straight-line” path:

$$u_t(z | \epsilon) = (1 - t) \cdot z + t \cdot \epsilon \quad (2)$$

Overall, the optimization objective of visual tokenization is formulated as minimizing the following flow-matching loss:

$$\mathcal{L}_{FM} = \mathbb{E}_{t, p_t(z|\epsilon), p(\epsilon)} \|\psi_{\Theta}(z_t, t, \mathbf{V}^2) - u_t(z | \epsilon)\|_2^2 \quad (3)$$

**Overview of V<sup>2</sup>Flow.** We begin by introducing the proposed visual vocabulary resampler (Sec. 2.2), which compresses visual content into a compact token sequence, with each token embedded in the vocabulary space of existing LLMs. Next, in Sec. 2.3, we present our masked autoregressive flow-matching decoder, designed to ensure high-quality visual reconstruction. Fig. 2 illustrates the overview of the V<sup>2</sup>Flow tokenizer.

### 2.2. Visual Vocabulary Resampler

Building upon recent advances [3, 5], we incorporate RegStage blocks [29] alongside a spatial downsampler [31] to compress the input image  $X \in \mathbb{R}^{H \times W \times C}$  into a latent representation  $Z \in \mathbb{R}^{h \times w \times d_v}$ . Here,  $h = H/q$ ,  $w = W/q$ ,  $q$  is the spatial downsampling factor and  $d_v$  denotes the embedding dimension. We then flatten  $Z$  into an one-dimensional sequence  $Z_{1D} \in \mathbb{R}^{n \times d_v}$ , where  $n < thw$  reflects the compression.

To align each visual token  $z_{1D} \in Z_{1D}$  with the pretrained LLM vocabulary, we introduce a generator module  $\mathcal{G}(\cdot)$  in conjunction with the Gumbel-softmax technique [16, 20]. This generator maps each visual token to a soft categorical distribution on an existing LLM [8, 17, 49] vocabulary  $\mathbf{L} \in \mathbb{R}^{N_l \times d_l}$ , containing  $N_l$  items. Note that the vocabulary remains fixed throughout the optimization process to preserve consistent semantic grounding. Specifically, the soft categorical distribution for each visual token is computed as follows:

$$\alpha_k = \frac{\exp(\mathcal{G}(z_{1D})_k + g_k)}{\sum_{j=1}^{N_l} \exp(\mathcal{G}(z_{1D})_j + g_j)}, \quad \forall k \in \{1, 2, \dots, N_l\} \quad (4)$$

where  $g_k \sim \text{Gumbel}(0, 1)$  represents independently sampled Gumbel noise, and  $\mathcal{G}(\cdot) : \mathbb{R}^{1 \times d_v} \rightarrow \mathbb{R}^{1 \times N_l}$  produces probability logits across  $N_l$  categories.

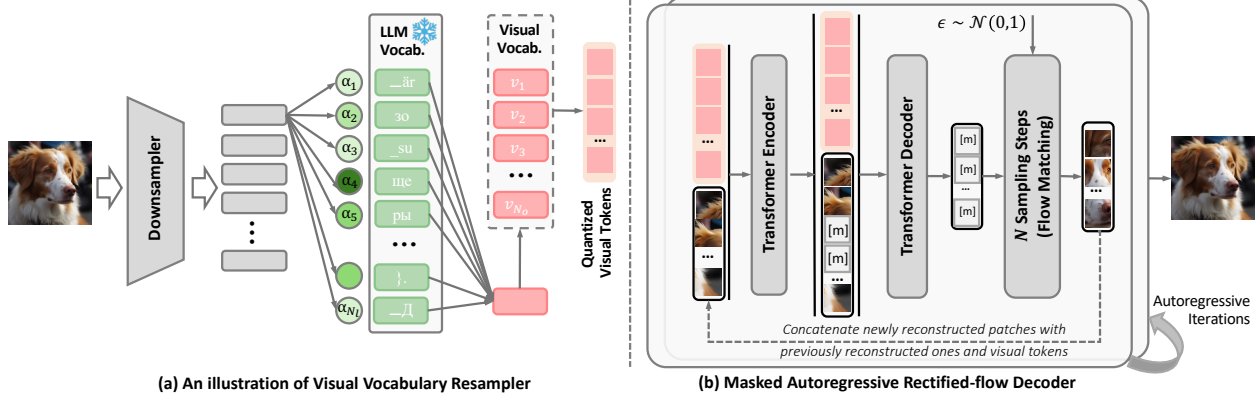
The resulting logits  $\alpha = (\alpha_1, \alpha_2, \dots, \alpha_{N_l})$  thus form a categorical distribution for each element  $z_{1D}$  over the LLM vocabulary. Each visual token is then embedded into the vocabulary space via  $\mathbf{v} = \alpha \cdot \mathbf{L}$ , where  $\mathbf{v}$  represents the *visual-vocabulary aligned* embedding. By directly operating in the LLM vocabulary space, our approach bridges visual and linguistic modalities while preserving crucial visual content.

Subsequently, each element  $\mathbf{v}$  is quantized by matching it to the closest code in the visual vocabulary codebook. We employ an exponentially moving average (EMA) scheme to update the codebook, consistent with findings that EMA improves convergence and training stability [43, 48].

### 2.3. Masked Autoregressive Rectified-Flow Decoder

Once visual elements are discretized into a feature space aligned with the vocabulary of pretrained LLMs, a critical challenge remains: how to reconstruct the original image with high-fidelity and detailed granularity. Drawing on recent advances in masked generative modeling, we introduce a transformer encoder-decoder architecture, augmented with a masking strategy, to facilitate flow-matching for high-quality visual reconstruction.

We first partition the input image  $X$  into  $N$  non-overlapping patches, forming a sequence  $\{x^0, x^1, \dots, x^N\}$ . A masking ratio  $\rho \in [0.7, 1.0]$  is then randomly selected (e.g.,  $\rho = 0.7$  masks 70% of the patches.). To incorporate contextual information from both the unmasked patches and



(a) An illustration of Visual Vocabulary Resampler

(b) Masked Autoregressive Rectified-flow Decoder

Figure 2. Overview of the V<sup>2</sup>Flow tokenizer, including ① Visual Vocabulary Resampler and ② Masked Autoregressive Rectified-Flow decoder. The first component is designed to compress visual content into a compact, one-dimensional discrete token sequence that are directly expressed within existing LLMs vocabularies. This enables seamless autoregressive visual generation **on top of** existing LLMs. Furthermore, the Masked Autoregressive Rectified-Flow decoder refines quantized tokens through a masked transformer encoder-decoder, producing visually enriched embeddings. These embeddings condition a tailored velocity field model to reconstruct the underlying visual content. Finally, a rectified-flow sampling strategy with autoregressive prediction offers flexibility in sequence length while preserving competitive reconstruction performance.

the quantized visual tokens, we concatenate them and feed the combined sequence into a transformer encoder.

For the reconstruction of masked patches, we initialize learnable mask tokens  $[m]$ , which are appended to the encoder output and passed into a transformer decoder. The decoder produces contextual embeddings for masked tokens  $[m]$ . These embeddings serve as conditioning signals for the velocity network in Eq. (1). Formally, the reconstruction process of masked patches is formulated as follows:

$$p(x_{0:t}^j | [m]) = p(x_t^j) \prod_{i=1}^t p(x_{(i-1)\Delta t}^j | z_{i\Delta t}^j, [m], t) \quad (5)$$

where  $j \in \Omega$  denotes the set of masked patches. The notation  $p(x_{0:t}^j | [m])$  represents that recovering target visual content from noised inputs  $x_t^j = \epsilon$ , conditioned on masked patches  $[m]$ ;  $\Delta t$  is the time-step size. Since the masked patches  $[m]$  already capture semantically rich visual representations through masked image modeling, we find that a lightweight MLP suffices to achieve high-fidelity visual reconstruction. This design simplifies the search for an optimal probabilistic path in the flow-matching process.

**Rectified-flow Sampling Stage.** At sampling time, we employ an autoregressive “next set-of-tokens prediction” scheme akin to MAR [22], progressively decreasing the masking ratio from 1.0 to 0 via a cosine schedule. At the initial iteration, with a masking ratio of 1.0, only the quantized visual tokens are fed into the transformer encoder-decoder, and a subset of tokens is randomly selected for reconstruction. In subsequent iterations, the newly reconstructed patches are concatenated with previously reconstructed patches and the

quantized visual tokens, then fed back into the encoder-decoder, continuing to reconstruct the next subset of masked patches. The overall sampling process follows:

$$p(\mathbf{x}^1, \dots, \mathbf{x}^K) = \begin{cases} \prod_{k=1}^K p(\mathbf{x}^k | \mathbf{V}^2), & k = 1 \\ \prod_{k=1}^K p(\mathbf{x}^k | \mathbf{V}^2, \mathbf{x}^1, \dots, \mathbf{x}^{k-1}), & k > 1 \end{cases} \quad (6)$$

Here,  $\mathbf{x}^k = \{x^i, x^{i+1}, \dots, x^j\}$  denotes the patches reconstructed at the  $k$ -th iteration, and  $\cup_k \mathbf{x}^k = \{x^0, x^1, \dots, x^N\}$  spans the full set of patches. Subsequently, the masked tokens produced by the decoder serve as conditioning signals for a lightweight velocity model to reconstruct the corresponding patches from noised samples. Classifier-free guidance is also incorporated during sampling, by interpolating between  $\psi_{\Theta}(z_t, t, \mathbf{V}^2)$  and its unconditional counterpart  $\psi_{\Theta}(z_t, t, \mathbf{D})$  via a scaling factor  $w$ ,

$$\tilde{\psi}_{\Theta}(z_t, t, \mathbf{V}^2) = w\psi_{\Theta}(z_t, t, \mathbf{V}^2) + (1-w)\psi_{\Theta}(z_t, t, \mathbf{D}) \quad (7)$$

where  $\mathbf{D}$  is a learnable dummy token under unconditional sampling. Overall, Algorithm 1 summarizes the sampling procedure of masked autoregressive rectified-flow decoder.

## 2.4. Equipped with LLM for Visual Generation

Fig. 3 illustrates the integration pipeline of our V<sup>2</sup>Flow tokenizer with LLMs for autoregressive visual generation. To facilitate seamless integration, we expand the existing LLM vocabulary with a set of visual-specific tokens, denoted as  $\langle v \rangle_{.0}, \langle v \rangle_{.1}, \langle v \rangle_{.2}, \dots, \langle v \rangle_{.N_0}$ , initialized directly using the codebook embeddings from our V<sup>2</sup>Flow tokenizer.

**Algorithm 1** Sampling Procedure of the Decoder

**Require:**  $V^2$  - Token sequence from the visual vocabulary resampler,  $steps$  - Autoregressive iteration steps

**Ensure:**  $\cup_k \mathbf{x}^k$  - Complete set of reconstructed patches

- 1:  $set \leftarrow \text{new set}()$
- 2: **for**  $k \leftarrow 0$  **to**  $steps$  **do**
- 3: Concatenate  $V^2$  with  $\{\mathbf{x}^0, \dots, \mathbf{x}^{k-1}\}$  and input into the transformer encoder.
- 4: Sample a masking ratio for iteration  $k$  from a cosine schedule in  $[1.0 \rightarrow 0]$ .
- 5: Reconstruct newly masked patches using classifier-free guidance in Eq. (7).
- 6:  $set.update(\mathbf{x}^k)$
- 7: **end for**
- 8: **return**  $\cup_k \mathbf{x}^k$

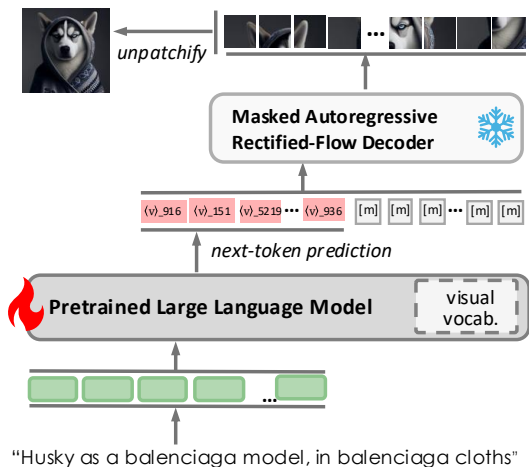


Figure 3. Pipeline for integrating  $V^2$ Flow tokenizer with pretrained LLMs for autoregressive visual generation.

Here, the notation  $N_v$  is the size of the visual vocabulary codebook. (See Sec. 2.2.)

During training, we formulate single-turn conversation data comprising text-image pairs, where the text prompt serves as the instruction, and the discrete visual tokens constitute the predictive target response. The LLM is optimized using an autoregressive training objective [24, 42], learning to predict the visual token sequence and determine appropriate stopping criteria.

At inference time, the pretrained LLM generates visual tokens autoregressively based on the input prompt until reaching a stopping token. Subsequently, the generated discretized visual tokens are fed into the  $V^2$ Flow decoder, where rectified-flow sampling reconstructs the original high-quality image, illustrated in Algorithm 1.

VQ-Tokenizer	Tokens	Codebook	ImageNet-1K		
			PSNR $\uparrow$	SSIM $\uparrow$	LPIPS $\downarrow$
<b>Resolution 256 <math>\times</math> 256:</b>					
Taming-VQGAN [9]	16 $\times$ 16	16,384	19.68	0.50	0.29
IBQ [33]	16 $\times$ 16	16,384	21.25	0.58	0.23
LlamaGen [36]	16 $\times$ 16	16,384	20.86	0.57	0.24
TiTok [55]	64	4,096	18.65	0.44	0.34
TiTok [55]	128	4,096	19.97	0.51	0.28
TiTok [55]	256	4,096	21.44	0.59	0.24
Open-MAGVIT2 [26]	16 $\times$ 16	262,144	21.76	0.60	0.21
Cosmos-DI [1]	16 $\times$ 16	64,000	20.38	0.52	0.28
$V^2$ Flow	256	16,384	<b>22.37</b>	<b>0.65</b>	<b>0.20</b>
<b>Resolution 512 <math>\times</math> 512:</b>					
Taming-VQGAN [9]	32 $\times$ 32	16,384	21.73	0.58	0.29
IBQ [33]	32 $\times$ 32	16,384	23.33	0.64	0.23
LlamaGen [36]	32 $\times$ 32	16,384	23.02	0.64	0.24
Open-MAGVIT2 [26]	32 $\times$ 32	262,144	<b>23.80</b>	0.65	0.22
Cosmos-DI [1]	32 $\times$ 32	64,000	22.57	0.61	0.27
$V^2$ Flow	1024	16,384	<u>23.28</u>	<b>0.65</b>	<b>0.22</b>

Table 1. Quantitative comparison with prior arts VQ-tokenizers at resolution 256  $\times$  256 and 512  $\times$  512 on ImageNet-1K test subset. Evaluation metrics including PSNR [15], SSIM [57] and LPIPS [44] are reported.

### 3. Experiments

#### 3.1. Experimental Settings

**Datasets.** For training the image tokenizer, we exclusively utilize the ImageNet training split [6]. The reconstruction performance is then evaluated on the ImageNet-1K test subset, which contains 100,000 images. Evaluations are conducted at two distinct resolutions: 256  $\times$  256 and 512  $\times$  512 pixels, enabling a comprehensive analysis of the model’s performance across varying image scales.

For the autoregressive text-conditioned image generation, the training dataset comprises approximately 6M image-text pairs from JourneyDB [35] and LAION-HD [32]. All images are center-cropped and resized proportionally to a resolution of 512  $\times$  512 pixels.

**Implementation Details.** To achieve autoregressive text-conditioned image generation, we employ the LLaMA2-7B language decoder [42] as our visual generative backbone. At the training stage, we empirically select a global batch size of 1,024 and a learning rate of 2e-5, training the model for 10 epochs. Consistent with LLaVA [24], we use the Adam optimizer without weight decay, applying a cosine learning rate schedule with a warm-up ratio of 3%. For implementation details of training  $V^2$ Flow tokenizer, please refer to the **supplementary material**.

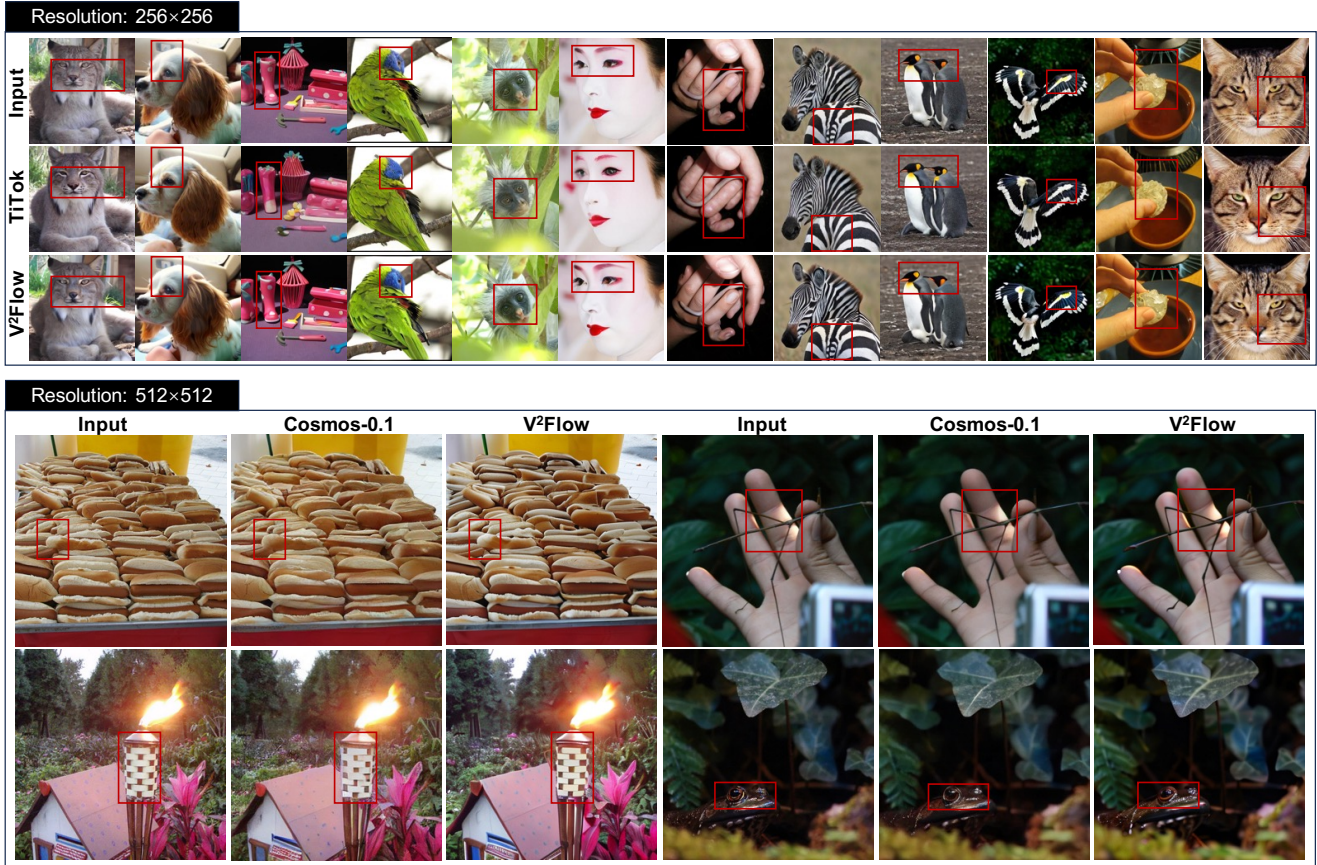


Figure 4. Qualitative comparisons of reconstruction quality on the ImageNet-1K test subset, comparing V<sup>2</sup>Flow against TiTok [55] at resolution 256×256 and the CosMos-Discrete [1] at resolution 512×512. For resolution 256 × 256, both V<sup>2</sup>Flow and TiTok [55] compress the input image into an one-dimensional sequence of 256 tokens, yet V<sup>2</sup>Flow reconstructs images with finer details. At resolution 512×512, compared to CosMos which compresses input images into 2D grid latents, V<sup>2</sup>Flow still achieves superior reconstruction quality.

ImageNet 256×256	Autoencoder	PSNR ↑	SSIM ↑	LPIPS ↓
64 tokens	TiTok [55]	18.65	0.44	0.34
	V <sup>2</sup> Flow	<b>20.41</b>	<b>0.52</b>	<b>0.26</b>
128 tokens	TiTok [55]	19.97	0.51	0.28
	V <sup>2</sup> Flow	<b>22.08</b>	<b>0.63</b>	<b>0.21</b>
256 tokens	TiTok [55]	21.44	0.59	0.24
	V <sup>2</sup> Flow	<b>22.37</b>	<b>0.65</b>	<b>0.20</b>

Table 2. Comparison of reconstruction quality with the 1D TiTok tokenizer [55] on ImageNet 256×256 at various token lengths.

### 3.2. Results on Reconstruction Quality

**Quantitative Results.** Tab. 1 summarizes the average quantitative metrics of our tokenizer on ImageNet-1K test subset of resolution 256 × 256 and 512 × 512. For ImageNet 256 × 256 results, ours tokenizer achieves state-of-the-art performance in all the metrics compared to prior arts. More importantly, even with a lower codebook size compared

DDIM	Rectified-Flow	CFG	PSNR ↑	SSIM ↑	LPIPS ↓
	✓		21.44	0.59	0.24
	✓	✓	<b>22.37</b>	<b>0.65</b>	<b>0.20</b>
✓		✓	22.23	0.64	0.20

Table 3. Ablation study of sampling strategy including classifier-free guidance (CFG) and different sampling strategy in the masked autoregressive decoder.

to the competitive Open-MAGVIT2 [26] ( from 16,384 to 262,144), our tokenizer improves over Open-MAGVIT2 by a large margin. For ImageNet 512 × 512 results, our tokenizer consistently achieves the competitive results compared to prior arts. These quantitative results confirm that our tokenizer can effectively represent visual content within the vocabulary space of pretrained LLMs, and accurately reconstruct original images while preserving pivotal details.

**Qualitative Analysis.** In Fig. 5, we compare reconstruction results on the ImageNet-1K test subset, evaluating our

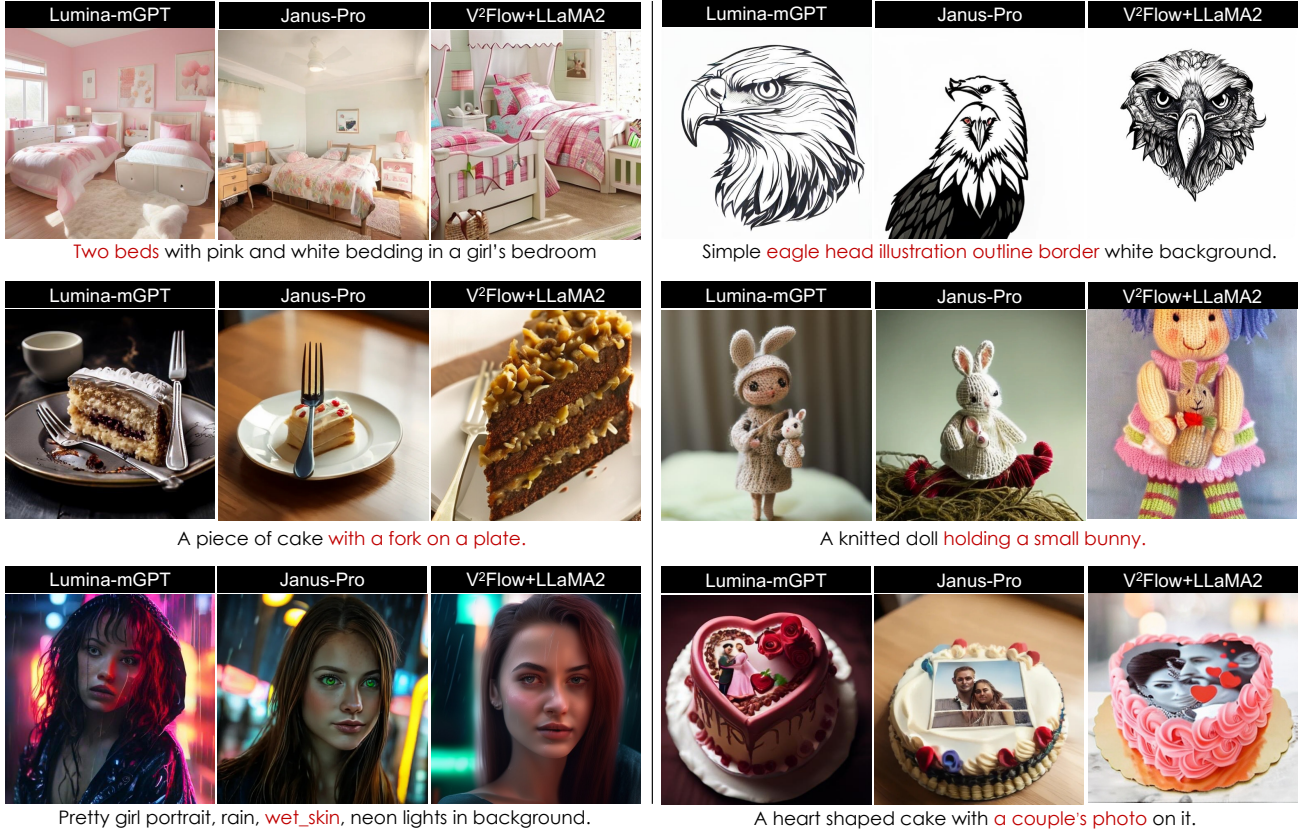


Figure 5. Qualitative results of text-conditioned image generation. We compare our approach against recent state-of-the-art autoregressive models, including Janus-Pro-7B [4] and Lumina-mGPT-7B [23]. All images are generated at a resolution of 512×512.

tokenizer against the competitive 1D tokenizer TiTok [55] at a  $256 \times 256$  resolution and the 2D CosMos tokenizer [1] at a  $512 \times 512$  resolutions, respectively. The visualization clearly indicates that our tokenizer more faithfully restore critical visual details that are lost in the reconstruction results of the competing tokenizers at both resolutions. These findings underscore the effectiveness of our tokenizer in preserving fine-grained visual content, highlighting its superior reconstruction fidelity.

**Flexibility in Tokenization Length.** A key advantage of our proposed masked autoregressive rectified-flow decoder is its ability to tokenize visual content at varying sequence lengths while preserving robust reconstruction performance. In Tab. 2, we compare the reconstruction results across different token lengths against the state-of-the-art TiTok tokenizer [55] on the ImageNet-1k test set at a resolution of  $256 \times 256$ . The experimental findings reveal that our method consistently outperforms TiTok across three different token sequence lengths. Notably, even with only 128 tokens, our approach surpasses TiTok’s reconstruction performance at 256 tokens, underscoring the efficiency and flexibility of the rectified-flow decoder.



**Ablation study of sampling strategy.** In Tab. 3, we first analyze the effect of classifier-free guidance during the masked autoregressive sampling stage. Quantitative results show that integrating classifier-free guidance achieves gains of 0.93 and 0.06 in PSNR and SSIM metrics. In addition, we examine the sensitivity of our tokenizer to different probability distribution modeling paradigms. When substituting the rectified-flow formulation with DDIM [34], our approach maintains competitive reconstruction quality. This confirms the robustness of the sampling strategy across different probability distribution modeling paradigms.

### 3.3. Results on Text-to-Image Generation

**Qualitative Analysis.** Fig. 5 provides a qualitative comparison of our text-to-image generation results against two state-of-the-art autoregressive models, Janus-Pro-7B [4] and Lumina-mGPT-7B [23]. The visualization illustrates that our V<sup>2</sup>Flow tokenizer, integrated with the LLaMA2-7B language model [42], more precisely captures semantic details from textual prompts. Consequently, our method achieves competitive generation quality, consistently producing coherent and contextually relevant images.



Figure 6. Analysis of the temperature hyperparameter during the autoregressive sampling process.

**Temperature of Autoregressive Sampling.** In Fig. 6, we present an analysis of the temperature hyperparameter during the autoregressive sampling process. We observe that appropriately tuned temperatures enhance diversity and introduce beneficial variability in the generated images. However, excessively high temperatures can compromise image coherence, resulting in semantically inconsistent or fragmented outcomes.

## 4. Related Works

**Visual Quantization.** VQ-VAE [43] stands as a pivotal work in the field of image quantization [21, 28, 51]. VQ-GAN [51] further refines this approach by incorporating adversarial and perceptual losses to capture more precise visual elements. Subsequent methods, including RQ-VAE [21] and MoVQ, [58] explore multiple vector quantization steps per latent embedding. MAGVIT-v2 [53] and FSQ [27] introduce lookup-free quantization strategies, leading to large visual codebooks and expressive representations. TiTok [55] adopts a masked transformer encoder-decoder to tokenize images at resolution  $256 \times 256$  into an one-dimensional sequence of 32 discrete tokens only.

Despite advances, the latent distributions of quantized visual tokens diverge significantly from those of text. The disparities between two modalities impose considerable challenges for autoregressive modeling. Although recent efforts [54, 61] address this by utilizing a LLM’s fixed vocabulary as the visual codebook, aligning visual and linguistic modalities more directly, the resulting tokens typically preserve the intrinsic two-dimensional structure of images. Consequently, autoregressive models must predict visual tokens in a line-by-line manner, deviating from the one-dimensional text-processing approach used by existing LLMs.

**Autoregressive Visual Generation.** Most existing autoregressive visual generation models [4, 8, 23, 36, 39, 41, 59] primarily focus on a sequential pixel-by-pixel process. Chameleon [39] simultaneously addresses image captioning and generation within a unified Transformer framework. Janus [4] decouples visual encoding into separate pathways yet employs a single transformer for multimodal

understanding and generation. Lumina-mGPT [23] captures extensive multimodal capabilities by applying a next-token prediction objective over interleaved text-image sequences. Transfusion [59] integrates next-token prediction for text with diffusion-based generation for images, unifying discrete and continuous modalities in one system. LlamaGen [36], built on vanilla autoregressive models, deliberately avoids visual inductive biases, instead advancing image generation through proper scaling. However, a fundamental challenge remains: these approaches typically convert two-dimensional images into one-dimensional sequences via a raster-scan ordering, limiting their ability to capture global structure. VAR [41] attempts to address this concern by reframing autoregressive visual generation as a coarse-to-fine “next-scale” or “next-resolution” prediction process. However, it remains susceptible to error accumulation when predicting multiple tokens in parallel.

In contrast, our V<sup>2</sup>Flow tokenizer compresses visual content into discrete token sequences that support superior reconstruction performance while maintaining both semantic and structural alignment with text representations in existing LLMs. This alignment facilitates autoregressive visual generation directly on top of existing LLMs.

**Comparison between V<sup>2</sup>Flow and MAR.** Our proposed Masked Autoregressive Rectified-Flow decoder within V<sup>2</sup>Flow shares conceptual ground with MAR [22]. However, beyond implementation differences, e.g., our adoption of a more efficient Rectified-Flow sampling strategy instead of MAR’s vanilla DDPM, we introduce a crucial conceptual advancement by capturing cross-modal mappings explicitly. We leverage masked image modeling to learn powerful contextual priors, facilitating detailed visual reconstructions guided by compact textual conditioning signals. This enables more effective integration of visual and textual modalities and paves the way toward a unified autoregressive framework for multimodal generation.

## 5. Conclusion

In this work, we introduce V<sup>2</sup>Flow tokenizer, a vector-quantized visual tokenizer with two core designs. First, we propose a visual vocabulary resampler transforming visual content into a compact token sequence expressed within pretrained LLM’s vocabulary space. This facilitates seamless integration into pretrained LLMs for autoregressive visual generation. Second, we develop masked autoregressive rectified-flow decoder in tandem with “next set-of-tokens” sampling strategy. This facilitates visual tokenization at varying sequence lengths while preserving robust and competitive reconstruction performance. Experimental results show that our V<sup>2</sup>Flow achieves competitive reconstruction performance compared to mainstream VQ-based tokenizers and effectively advances autoregressive visual generation.



## References

- [1] Niket Agarwal, Arslan Ali, Maciej Bala, Yogesh Balaji, Erik Barker, Tiffany Cai, Prithvijit Chattopadhyay, Yongxin Chen, Yin Cui, Yifan Ding, et al. Cosmos world foundation model platform for physical ai. *arXiv preprint arXiv:2501.03575*, 2025. 5, 6, 7
- [2] Jinze Bai, Shuai Bai, Yunfei Chu, Zeyu Cui, Kai Dang, Xiaodong Deng, Yang Fan, Wenbin Ge, Yu Han, Fei Huang, et al. Qwen technical report. *arXiv preprint arXiv:2309.16609*, 2023. 1
- [3] Junbum Cha, Wooyoung Kang, Jonghwan Mun, and Byungseok Roh. Honeybee: Locality-enhanced projector for multimodal llm. In *Proceedings of the IEEE/CVF Conference on Computer Vision and Pattern Recognition*, pages 13817–13827, 2024. 3
- [4] Xiaokang Chen, Zhiyu Wu, Xingchao Liu, Zizheng Pan, Wen Liu, Zhenda Xie, Xingkai Yu, and Chong Ruan. Januspro: Unified multimodal understanding and generation with data and model scaling. *arXiv preprint arXiv:2501.17811*, 2025. 7, 8
- [5] Zesen Cheng, Sicong Leng, Hang Zhang, Yifei Xin, Xin Li, Guanzheng Chen, Yongxin Zhu, Wenqi Zhang, Ziyang Luo, Deli Zhao, et al. Videollama 2: Advancing spatial-temporal modeling and audio understanding in video-llms. *arXiv preprint arXiv:2406.07476*, 2024. 1, 3
- [6] Jia Deng, Wei Dong, Richard Socher, Li-Jia Li, Kai Li, and Li Fei-Fei. Imagenet: A large-scale hierarchical image database. In *2009 IEEE conference on computer vision and pattern recognition*, pages 248–255. Ieee, 2009. 5
- [7] Runpei Dong, Chunrui Han, Yuang Peng, Zekun Qi, Zheng Ge, Jinrong Yang, Liang Zhao, Jianjian Sun, Hongyu Zhou, Haoran Wei, et al. Dreamllm: Synergistic multimodal comprehension and creation. *arXiv preprint arXiv:2309.11499*, 2023. 1
- [8] Abhimanyu Dubey, Abhinav Jauhri, Abhinav Pandey, Abhishek Kadian, Ahmad Al-Dahle, Aiesha Letman, Akhil Mathur, Alan Schelten, Amy Yang, Angela Fan, et al. The llama 3 herd of models. *arXiv preprint arXiv:2407.21783*, 2024. 1, 2, 3, 8
- [9] Patrick Esser, Robin Rombach, and Bjorn Ommer. Taming transformers for high-resolution image synthesis. In *Proceedings of the IEEE/CVF conference on computer vision and pattern recognition*, pages 12873–12883, 2021. 1, 5
- [10] Patrick Esser, Sumith Kulal, Andreas Blattmann, Rahim Entezari, Jonas Müller, Harry Saini, Yam Levi, Dominik Lorenz, Axel Sauer, Frederic Boesel, et al. Scaling rectified flow transformers for high-resolution image synthesis. In *Forty-first international conference on machine learning*, 2024. 2, 3
- [11] Rongyao Fang, Chengqi Duan, Kun Wang, Hao Li, Hao Tian, Xingyu Zeng, Rui Zhao, Jifeng Dai, Hongsheng Li, and Xihui Liu. Puma: Empowering unified mllm with multi-granular visual generation. *arXiv preprint arXiv:2410.13861*, 2024. 1
- [12] Yuying Ge, Sijie Zhao, Jinguo Zhu, Yixiao Ge, Kun Yi, Lin Song, Chen Li, Xiaohan Ding, and Ying Shan. Seed-x: Multimodal models with unified multi-granularity comprehension and generation. *arXiv preprint arXiv:2404.14396*, 2024. 1
- [13] Kaiming He, Xinlei Chen, Saining Xie, Yanghao Li, Piotr Dollár, and Ross Girshick. Masked autoencoders are scalable vision learners. In *Proceedings of the IEEE/CVF conference on computer vision and pattern recognition*, pages 16000–16009, 2022. 2
- [14] Jonathan Ho, Ajay Jain, and Pieter Abbeel. Denoising diffusion probabilistic models. *Advances in neural information processing systems*, 33:6840–6851, 2020. 1
- [15] Alain Hore and Djemel Ziou. Image quality metrics: Psnr vs. ssim. In *2010 20th international conference on pattern recognition*, pages 2366–2369. IEEE, 2010. 5
- [16] Eric Jang, Shixiang Gu, and Ben Poole. Categorical reparameterization with gumbel-softmax. *arXiv preprint arXiv:1611.01144*, 2016. 3
- [17] Albert Q Jiang, Alexandre Sablayrolles, Antoine Roux, Arthur Mensch, Blanche Savary, Chris Bamford, Devendra Singh Chaplot, Diego de las Casas, Emma Bou Hanna, Florian Bressand, et al. Mixtral of experts. *arXiv preprint arXiv:2401.04088*, 2024. 3
- [18] Diederik P Kingma. Auto-encoding variational bayes. *arXiv preprint arXiv:1312.6114*, 2013. 1
- [19] Dan Kondratyuk, Lijun Yu, Xiuye Gu, José Lezama, Jonathan Huang, Grant Schindler, Rachel Hornung, Vignesh Birodkar, Jimmy Yan, Ming-Chang Chiu, et al. Videopoet: A large language model for zero-shot video generation. *arXiv preprint arXiv:2312.14125*, 2023. 1
- [20] Matt J Kusner and José Miguel Hernández-Lobato. Gans for sequences of discrete elements with the gumbel-softmax distribution. *arXiv preprint arXiv:1611.04051*, 2016. 3
- [21] Doyup Lee, Chiheon Kim, Saehoon Kim, Minsu Cho, and Wook-Shin Han. Autoregressive image generation using residual quantization. In *Proceedings of the IEEE/CVF Conference on Computer Vision and Pattern Recognition*, pages 11523–11532, 2022. 1, 8
- [22] Tianhong Li, Yonglong Tian, He Li, Mingyang Deng, and Kaiming He. Autoregressive image generation without vector quantization. *Advances in Neural Information Processing Systems*, 37:56424–56445, 2024. 2, 4, 8
- [23] Dongyang Liu, Shitian Zhao, Le Zhuo, Weifeng Lin, Yu Qiao, Hongsheng Li, and Peng Gao. Lumina-mgpt: Illuminate flexible photorealistic text-to-image generation with multimodal generative pretraining. *arXiv preprint arXiv:2408.02657*, 2024. 7, 8
- [24] Haotian Liu, Chunyuan Li, Qingyang Wu, and Yong Jae Lee. Visual instruction tuning. *Advances in neural information processing systems*, 36:34892–34916, 2023. 5
- [25] Haotian Liu, Chunyuan Li, Qingyang Wu, and Yong Jae Lee. Visual instruction tuning. *Advances in neural information processing systems*, 36, 2024. 1
- [26] Zhuoyan Luo, Fengyuan Shi, Yixiao Ge, Yujiu Yang, Limin Wang, and Ying Shan. Open-magvit2: An open-source project toward democratizing auto-regressive visual generation. *arXiv preprint arXiv:2409.04410*, 2024. 5, 6
- [27] Fabian Mentzer, David Minnen, Eirikur Agustsson, and Michael Tschannen. Finite scalar quantization: Vq-vae made simple. *arXiv preprint arXiv:2309.15505*, 2023. 8

- [28] Zhiliang Peng, Li Dong, Hangbo Bao, Qixiang Ye, and Furu Wei. Beit v2: Masked image modeling with vector-quantized visual tokenizers. *arXiv preprint arXiv:2208.06366*, 2022. 8
- [29] Ilija Radosavovic, Raj Prateek Kosaraju, Ross Girshick, Kaiming He, and Piotr Dollár. Designing network design spaces. In *Proceedings of the IEEE/CVF conference on computer vision and pattern recognition*, pages 10428–10436, 2020. 3
- [30] Danilo Jimenez Rezende, Shakir Mohamed, and Daan Wierstra. Stochastic backpropagation and approximate inference in deep generative models. In *International conference on machine learning*, pages 1278–1286. PMLR, 2014. 1
- [31] Robin Rombach, Andreas Blattmann, Dominik Lorenz, Patrick Esser, and Björn Ommer. High-resolution image synthesis with latent diffusion models. In *Proceedings of the IEEE/CVF conference on computer vision and pattern recognition*, pages 10684–10695, 2022. 3
- [32] Christoph Schuhmann, Romain Beaumont, Richard Vencu, Cade Gordon, Ross Wightman, Mehdi Cherti, Theo Coombes, Aarush Katta, Clayton Mullis, Mitchell Wortsman, et al. Laion-5b: An open large-scale dataset for training next generation image-text models. *Advances in neural information processing systems*, 35:25278–25294, 2022. 5
- [33] Fengyuan Shi, Zhuoyan Luo, Yixiao Ge, Yujiu Yang, Ying Shan, and Limin Wang. Taming scalable visual tokenizer for autoregressive image generation. *arXiv preprint arXiv:2412.02692*, 2024. 1, 5
- [34] Jiaming Song, Chenlin Meng, and Stefano Ermon. Denoising diffusion implicit models. *arXiv preprint arXiv:2010.02502*, 2020. 1, 7
- [35] Keqiang Sun, Junting Pan, Yuying Ge, Hao Li, Haodong Duan, Xiaoshi Wu, Renrui Zhang, Aojun Zhou, Zipeng Qin, Yi Wang, et al. Journeydb: A benchmark for generative image understanding. *Advances in neural information processing systems*, 36:49659–49678, 2023. 5
- [36] Peize Sun, Yi Jiang, Shoufa Chen, Shilong Zhang, Bingyue Peng, Ping Luo, and Zehuan Yuan. Autoregressive model beats diffusion: Llama for scalable image generation. *arXiv preprint arXiv:2406.06525*, 2024. 1, 5, 8
- [37] Quan Sun, Qiyang Yu, Yufeng Cui, Fan Zhang, Xiaosong Zhang, Yueze Wang, Hongcheng Gao, Jingjing Liu, Tiejun Huang, and Xinlong Wang. Emu: Generative pretraining in multimodality. In *The Twelfth International Conference on Learning Representations*, 2023. 1
- [38] Quan Sun, Yufeng Cui, Xiaosong Zhang, Fan Zhang, Qiyang Yu, Yueze Wang, Yongming Rao, Jingjing Liu, Tiejun Huang, and Xinlong Wang. Generative multimodal models are in-context learners. In *Proceedings of the IEEE/CVF Conference on Computer Vision and Pattern Recognition*, pages 14398–14409, 2024. 1
- [39] Chameleon Team. Chameleon: Mixed-modal early-fusion foundation models, 2024. URL <https://arxiv.org/abs/2405.09818>, 9. 8
- [40] Chameleon Team. Chameleon: Mixed-modal early-fusion foundation models. *arXiv preprint arXiv:2405.09818*, 2024. 1
- [41] Keyu Tian, Yi Jiang, Zehuan Yuan, Bingyue Peng, and Liwei Wang. Visual autoregressive modeling: Scalable image generation via next-scale prediction. *arXiv preprint arXiv:2404.02905*, 2024. 8
- [42] Hugo Touvron, Thibaut Lavril, Gautier Izacard, Xavier Martinet, Marie-Anne Lachaux, Timothée Lacroix, Baptiste Rozière, Naman Goyal, Eric Hambro, Faisal Azhar, et al. Llama: Open and efficient foundation language models. *arXiv preprint arXiv:2302.13971*, 2023. 1, 2, 5, 7
- [43] Aaron Van Den Oord, Oriol Vinyals, et al. Neural discrete representation learning. *Advances in neural information processing systems*, 30, 2017. 3, 8
- [44] Zhou Wang, Alan C Bovik, Hamid R Sheikh, and Eero P Simoncelli. Image quality assessment: from error visibility to structural similarity. *IEEE transactions on image processing*, 13(4):600–612, 2004. 5
- [45] Chen Wei, Haoqi Fan, Saining Xie, Chao-Yuan Wu, Alan Yuille, and Christoph Feichtenhofer. Masked feature prediction for self-supervised visual pre-training. In *Proceedings of the IEEE/CVF conference on computer vision and pattern recognition*, pages 14668–14678, 2022. 2
- [46] Shitao Xiao, Yueze Wang, Junjie Zhou, Huaying Yuan, Xin-grun Xing, Ruiran Yan, Shuting Wang, Tiejun Huang, and Zheng Liu. Omnigen: Unified image generation. *arXiv preprint arXiv:2409.11340*, 2024. 1
- [47] Jinheng Xie, Weijia Mao, Zechen Bai, David Junhao Zhang, Weihao Wang, Kevin Qinghong Lin, Yuchao Gu, Zhijie Chen, Zhenheng Yang, and Mike Zheng Shou. Show-o: One single transformer to unify multimodal understanding and generation. *arXiv preprint arXiv:2408.12528*, 2024. 1
- [48] Wilson Yan, Yunzhi Zhang, Pieter Abbeel, and Aravind Srinivas. Videogpt: Video generation using vq-vae and transformers. *arXiv preprint arXiv:2104.10157*, 2021. 3
- [49] An Yang, Baosong Yang, Binyuan Hui, Bo Zheng, Bowen Yu, Chang Zhou, Chengpeng Li, Chengyuan Li, Dayiheng Liu, Fei Huang, et al. Qwen2 technical report. *arXiv preprint arXiv:2407.10671*, 2024. 3
- [50] Yuan Yao, Tianyu Yu, Ao Zhang, Chongyi Wang, Junbo Cui, Hongji Zhu, Tianchi Cai, Haoyu Li, Weilin Zhao, Zhihui He, et al. Minicpm-v: A gpt-4v level mllm on your phone. *arXiv preprint arXiv:2408.01800*, 2024. 1
- [51] Jiahui Yu, Xin Li, Jing Yu Koh, Han Zhang, Ruoming Pang, James Qin, Alexander Ku, Yuanzhong Xu, Jason Baldridge, and Yonghui Wu. Vector-quantized image modeling with improved vqgan. *arXiv preprint arXiv:2110.04627*, 2021. 8
- [52] Lijun Yu, Yong Cheng, Kihyuk Sohn, José Lezama, Han Zhang, Huiwen Chang, Alexander G Hauptmann, Ming-Hsuan Yang, Yuan Hao, Irfan Essa, et al. Magvit: Masked generative video transformer. In *Proceedings of the IEEE/CVF Conference on Computer Vision and Pattern Recognition*, pages 10459–10469, 2023. 1
- [53] Lijun Yu, José Lezama, Nitesh B Gundavarapu, Luca Versari, Kihyuk Sohn, David Minnen, Yong Cheng, Vignesh Birodkar, Agrim Gupta, Xiuye Gu, et al. Language model beats diffusion–tokenizer is key to visual generation. *arXiv preprint arXiv:2310.05737*, 2023. 1, 8
- [54] Lijun Yu, Yong Cheng, Zhiruo Wang, Vivek Kumar, Wolfgang Macherey, Yanping Huang, David Ross, Irfan Essa,

- Yonatan Bisk, Ming-Hsuan Yang, et al. Spae: Semantic pyramid autoencoder for multimodal generation with frozen llms. *Advances in Neural Information Processing Systems*, 36, 2024. 8
- [55] Qihang Yu, Mark Weber, Xueqing Deng, Xiaohui Shen, Daniel Cremers, and Liang-Chieh Chen. An image is worth 32 tokens for reconstruction and generation. *arXiv preprint arXiv:2406.07550*, 2024. 2, 5, 6, 7, 8
- [56] Hang Zhang, Xin Li, and Lidong Bing. Video-llama: An instruction-tuned audio-visual language model for video understanding. *arXiv preprint arXiv:2306.02858*, 2023. 1
- [57] Richard Zhang, Phillip Isola, Alexei A Efros, Eli Shechtman, and Oliver Wang. The unreasonable effectiveness of deep features as a perceptual metric. In *Proceedings of the IEEE conference on computer vision and pattern recognition*, pages 586–595, 2018. 5
- [58] Chuanxia Zheng, Tung-Long Vuong, Jianfei Cai, and Dinh Phung. Movq: Modulating quantized vectors for high-fidelity image generation. *Advances in Neural Information Processing Systems*, 35:23412–23425, 2022. 1, 8
- [59] Chunting Zhou, Lili Yu, Arun Babu, Kushal Tirumala, Michihiro Yasunaga, Leonid Shamis, Jacob Kahn, Xuezhe Ma, Luke Zettlemoyer, and Omer Levy. Transfusion: Predict the next token and diffuse images with one multi-modal model. *arXiv preprint arXiv:2408.11039*, 2024. 1, 8
- [60] Deyao Zhu, Jun Chen, Xiaoqian Shen, Xiang Li, and Mohamed Elhoseiny. Minigpt-4: Enhancing vision-language understanding with advanced large language models. *arXiv preprint arXiv:2304.10592*, 2023. 1
- [61] Lei Zhu, Fangyun Wei, and Yanye Lu. Beyond text: Frozen large language models in visual signal comprehension. In *Proceedings of the IEEE/CVF Conference on Computer Vision and Pattern Recognition*, pages 27047–27057, 2024. 8